power, given by the Curzon-Ahlborn (*26*) formula $\eta_{\mathrm{CA}} = 1 - \sqrt{T_1/T_2}$ = 1.9%, reflects that the current trap parameters do not correspond to the optimal point (*14*). The performance of future single-ion heat engines could be improved by redesigning the geometry of the trap to have cycles with a higher range of frequencies ω_r (see Fig. 4B). This could be achieved by increasing either the angle of the taper or the absolute radial trap frequencies.

We have demonstrated a realization of a heat engine whose working agent is a single atom. This classical device offers a broad platform for future experiments investigating, for instance, machines coupled to nonthermal reservoirs (*27*) or single-ion refrigerators and pumps (*28*). Moreover, the quantum regime ($k_B T \approx \hbar\omega_r$) could be reached by replacing Doppler cooling by electromagnetically induced transparency cooling or side-band cooling (*10*), as in the recent verification of the quantum Jarzynski equality (*29*). In the quantum domain, dark-state thermometry could be replaced by side-band spectroscopy, again allowing for the determination of the cycle of the engine and thus its power and efficiency. Such a system would permit the study of the performance of small quantum machines (*30*, *31*) and the exploration of genuine quantum effects in thermodynamics, such as quantum coherences (*32*) and correlations (*33*), as well as the testing of predictions of quantum resource theory (*34*, *35*).

REFERENCES AND NOTES

1. Y. A. Çengel, M. A. Boles, M. Kanoğlu, *Thermodynamics: An Engineering Approach* (McGraw-Hill, ed. 8, 2014).
2. S. Whalen, M. Thompson, D. Bahr, C. Richards, R. Richards, *Sens. Actuators A* **104**, 290–298 (2003).
3. P. Steeneken *et al.*, *Nat. Phys.* **7**, 354–359 (2011).
4. J.-P. Brantut *et al.*, *Science* **342**, 713–715 (2013).
5. V. Blickle, C. Bechinger, *Nat. Phys.* **8**, 143–146 (2012).
6. I. A. Martínez *et al.*, *Nat. Phys.* **12**, 67–70 (2016).
7. T. Hugel *et al.*, *Science* **296**, 1103–1106 (2002).
8. R. P. Feynman, *Eng. Sci.* **23**, 22 (1960).
9. J. Roßnagel, K. N. Tolazzi, F. Schmidt-Kaler, K. Singer, *New J. Phys.* **17**, 045004 (2015).
10. D. Leibfried, R. Blatt, C. Monroe, D. Wineland, *Rev. Mod. Phys.* **75**, 281–324 (2003).
11. R. Blatt, D. Wineland, *Nature* **453**, 1008–1015 (2008).
12. J. F. Poyatos, J. I. Cirac, P. Zoller, *Phys. Rev. Lett.* **77**, 4728–4731 (1996).
13. C. J. Myatt *et al.*, *Nature* **403**, 269–273 (2000).
14. O. Abah *et al.*, *Phys. Rev. Lett.* **109**, 203006 (2012).
15. H. J. Metcalf, P. van der Straten, *Laser Cooling and Trapping* (Springer, 1999).
16. J. I. Cirac, R. Blatt, P. Zoller, W. D. Phillips, *Phys. Rev. A* **46**, 2668–2681 (1992).
17. J. I. Cirac, M. Lewenstein, P. Zoller, *Phys. Rev. Lett.* **72**, 2977–2980 (1994).
18. H. C. Nägerl, D. Leibfried, F. Schmidt-Kaler, J. Eschner, R. Blatt, *Opt. Express* **3**, 89–96 (1998).
19. B. Lin, J. Chen, *Phys. Rev. E* **67**, 046105 (2003).
20. T. Peters, B. Wittrock, F. Blatt, T. Halfmann, L. P. Yatsenko, *Phys. Rev. A* **85**, 063416 (2012).
21. S. Knünz *et al.*, *Phys. Rev. A* **85**, 023427 (2012).
22. G. S. Agarwal, S. Chaturvedi, *Phys. Rev. E* **88**, 012130 (2013).
23. K. Brandner, K. Saito, U. Seifert, *Phys. Rev. X* **5**, 031019 (2015).
24. J. R. Taylor, *Classical Mechanics* (University Science, Sausalito, CA, 2005).
25. L. D. Landau, E. M. Lifschitz, *Statistical Physics* (Elsevier, 1980).
26. F. Curzon, B. Ahlborn, *Am. J. Phys.* **43**, 22 (1975).
27. J. Roßnagel, O. Abah, F. Schmidt-Kaler, K. Singer, E. Lutz, *Phys. Rev. Lett.* **112**, 030602 (2014).
28. B. Lin, J. Chen, *Phys. Rev. E* **68**, 056117 (2003).
29. S. An *et al.*, *Nat. Phys.* **11**, 193–199 (2014).
30. N. Linden, S. Popescu, P. Skrzypczyk, *Phys. Rev. Lett.* **105**, 130401 (2010).
31. R. Kosloff, A. Levy, *Annu. Rev. Phys. Chem.* **65**, 365–393 (2014).
32. M. O. Scully, M. S. Zubairy, G. S. Agarwal, H. Walther, *Science* **299**, 862–864 (2003).
33. R. Dillenschneider, E. Lutz, *Europhys. Lett.* **88**, 50003 (2009).
34. F. G. Brandão, M. Horodecki, J. Oppenheim, J. M. Renes, R. W. Spekkens, *Phys. Rev. Lett.* **111**, 250404 (2013).
35. M. Horodecki, J. Oppenheim, *Nat. Commun.* **4**, 2059 (2013).

ACKNOWLEDGMENTS

We thank Princeton Instruments for the loan of the ICCD camera and S. Deffner for fruitful discussions. Supported by the German Research Foundation (grant "Einzelionenwärmekraftmaschine"), the Volkswagen Foundation (grant "Atomic Nano-Assembler"), European Union (EU) COST action MP1209, and the EU Collaborative Project TherMiQ (grant agreement 618074). The data presented in this report are available upon request to K.S.

14 October 2015; accepted 4 March 2016
10.1126/science.aad6320

ORGANOMETALLICS

Pre-transmetalation intermediates in the Suzuki-Miyaura reaction revealed: The missing link

Andy A. Thomas and Scott E. Denmark*

Despite the widespread application of Suzuki-Miyaura cross-coupling to forge carbon-carbon bonds, the structure of the reactive intermediates underlying the key transmetalation step from the boron reagent to the palladium catalyst remains uncertain. Here we report the use of low-temperature rapid injection nuclear magnetic resonance spectroscopy and kinetic studies to generate, observe, and characterize these previously elusive complexes. Specifically, this work establishes the identity of three different species containing palladium-oxygen-boron linkages, a tricoordinate boronic acid complex, and two tetracoordinate boronate complexes with 2:1 and 1:1 stoichiometry with respect to palladium. All of these species transfer their boron-bearing aryl groups to a coordinatively unsaturated palladium center in the critical transmetalation event.

Palladium-catalyzed cross-coupling reactions have fundamentally changed the practice of organic synthesis. These reactions forge carbon-carbon bonds through the migration of a carbon-based substituent from a main group element to palladium, as exemplified by the Kumada-Tamao-Corriu (Mg) (*1*), Suzuki-Miyaura (B) (*2*), Stille-Migita-Kosugi (Sn) (*3*), Negishi (Zn) (*4*), and Hiyama-Denmark (Si) (*5*) reactions. The Nobel Prize–sharing Suzuki-Miyaura reaction (*6*) is currently the premier cross-coupling process and has been widely applied in organic (*7*), medicinal (*8*), and materials (*9*) chemistry. It is also frequently used in the industrial syntheses of fine chemicals (*10*) and pharmaceuticals (*11*) because of its demonstrated reliability, its functional group compatibility, and the low cost and ease of handling of a wide variety of commercially available boron-based reagents.

Despite the preeminent status of the Suzuki-Miyaura reaction, a fundamental understanding of the critical migratory transmetalation event from boron to palladium has thus far been lacking (*12*–*18*). For decades, chemists have considered two pathways (path A and path B in Fig. 1) that differ in the role that the hydroxide ion plays in initiating the transmetalation event. Path A proceeds through the combination of a negatively charged aryltrihydroxyboronate (compound **1**) and a palladium halide complex (**2**), which form a hypothetical intermediate containing a Pd-O-B unit (**3**). The alternative path B proceeds through the combination of a neutral arylboronic acid (**4**) and a palladium hydroxide complex (formed through the displacement of the organopalladium halide by hydroxide; **5**), ultimately converging to the same intermediate **3**, which is then poised to transfer the aryl group to palladium in an intramolecular β-aryl elimination step, followed by reductive elimination (Fig. 1). Species such as **3** represent the missing link between the starting organoboron reagents and the diorganopalladium intermediates that are known to afford cross-coupling products.

The role of the base in the Suzuki-Miyaura reaction was investigated initially by the Soderquist laboratory (*12*) and, more recently, by the laboratories of Hartwig (*13*), Amatore and Jutand (*14*–*16*), and Schmidt (*17*, *18*). The kinetic analysis in (*13*) established that path B is favored over path A by more than four orders of magnitude, a conclusion that is reinforced by the extensive kinetic studies in (*14*–*16*), which clearly identified multiple antagonistic roles for the hydroxide ion. Although nuclear magnetic resonance (NMR) spectroscopic and kinetic studies have

---

Roger Adams Laboratory, Department of Chemistry, University of Illinois, Urbana, IL 61801, USA.
***Corresponding author. E-mail: sdenmark@illinois.edu**

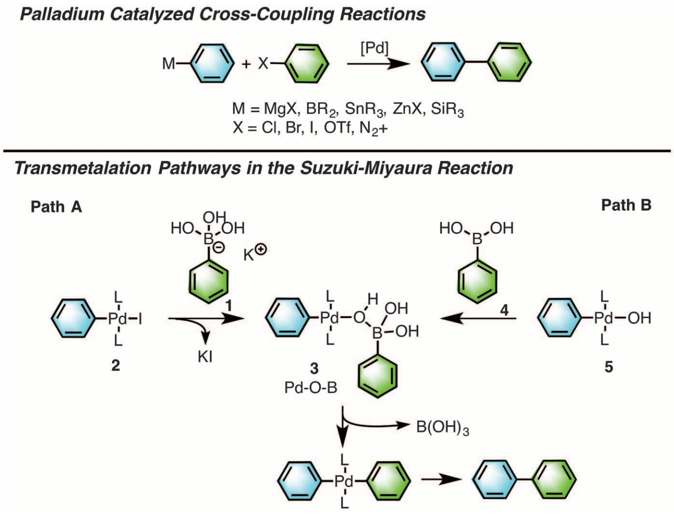

Fig. 1. Palladium-catalyzed cross-coupling reactions and proposed transmetalation pathways in the Suzuki-Miyaura process. R indicates an organic group. Compound numbers are shown in bold in the lower panel.

provided independent evidence for these pathways, the actual composition and structure of the transmetalation precursors have not been unambiguously defined, despite being widely assumed. Because of the transient nature of these intermediates, traditional methods (e.g., electrospray mass spectrometry and traditional NMR spectroscopy) have proven incapable of characterizing highly reactive intermediates such as **3** (*19*, *20*). Although the intermediacy of a species containing a Pd-O-B linkage has been proposed, its observation and characterization have eluded chemists for over 30 years (*21*). A recent review by Lennox and Lloyd-Jones (*22*) states that "[t]he barrier of this process was predicted computationally to be low (14–22 kcal mol^{-1}), suggesting specialist techniques will need to be applied to detect and confirm the identity of [**3**] experimentally." One such technique that has proven valuable for providing structural and kinetic data in similar mechanistic studies is rapid injection NMR (RI-NMR) (*23*).

Aided by the RI-NMR apparatus developed in our laboratories (*24*), we have undertaken the generation and structural and kinetic characterization of these elusive intermediates. We hypothesized that combining stoichiometric amounts of arylpalladium complex *trans*-(i-$Pr_3P)_2$(4-FC_6H_4)Pd(OH) (**6**) with 4-fluorophenylboronic acid (**7**) (Fig. 2, route 1), or *trans*-(i-$Pr_3P)_2$(4-FC_6H_4)Pd(I) (**8**) with thallium 4-fluorophenylboronate (**10**) (Fig. 2, route 2), should converge on a species whose structure and kinetic competence can be examined. The choice of triisopropylphosphine (i-Pr_3P) was critical to allow the preparation of discrete, stable precursors and also to facilitate structural assignments (*25*, *26*).

The synthesis in route 1 involved the addition of a tetrahydrofuran-d_8 (THF-d_8) solution of 4-fluorophenylboronic acid (**7**) to a THF-d_8 solution of *trans*-(i-$Pr_3P)_2$(4-FC_6H_4)Pd(OH) (**6**), together with 2.0 equivalents of i-Pr_3P, at –78°C (Fig. 2). Although no new species were observed at –60°C, warming the solution to –30°C resulted in the quantitative conversion of compounds **6** and **7** to a new species. The combination of one- and two-dimensional NMR spectroscopic techniques executed at –30°C led to the structural elucidation of the newly formed species as complex **11**, containing a Pd-O-B linkage (supplementary materials, figs. S1 to S10).

The coordination geometry was assigned to a *trans*-bisphosphino square planar palladium complex. This assignment was based on the observation of the ^{13}C NMR signal (PCH) at 25.38 parts per million (ppm) as an apparent triplet ($J_{P\text{-}C}$ = 10 Hz; J is the coupling constant between the phosphorus and carbon atoms) attributable to virtual coupling (*27*) and the ^{31}P NMR signal at 29.98 ppm (a solitary singlet), which is shifted slightly upfield compared with the corresponding resonance of **6** at 33.00 ppm (figs. S2 and S4).

The bonding connectivity of complex **11** was established by the observation of strong through-space interactions [nuclear Overhauser effect (NOE) spectroscopy] of both H_b and H_d (hydrogens in the b and d positions) with the methyl hydrogens on the i-Pr_3P group (Fig. 2, blue arrows, and fig. S10). In addition, cross peaks between the B-OH group and the *ipso*-carbon [C(1)]–bearing boron ($^3J_{BOH\text{-}C(1)}$) were observed in the heteronuclear multiple-bond correlation (HMBC) spectrum (Fig. 2, red bonds, and fig. S9). The resonances for H_a and H_b (Fig. 2, blue aryl) and H_c and H_d (green aryl) are shifted slightly downfield (+0.07 to +0.16 ppm) in complex **11**, compared with substrates **6** and **7** (table S1). The resonances for the fluorine atoms in **11** [F_a (blue aryl) and F_b (green aryl)] are both shifted upfield relative to those associated with **6** and **7**, but the change was much more pronounced for F_b (–4.54 to –0.91 ppm), which facilitated their identification.

Most importantly, the boron atom in complex **11** was assigned to a tricoordinate geometry [6-B-3 (*28*)] on the basis of the ^{11}B NMR signal, which appeared as a broad singlet at 29 ppm (table S1)—well within the chemical shift regime for 6-B-3 boron compounds (*29*). Related 6-B-3 complexes of arylboronic and diarylborinic acids with Pt and Rh have been synthesized and exhibit ^{11}B NMR resonances similar to that of **11** (*30*, *31*).

To provide additional evidence for the structure of **11**, an independent synthesis was carried out (route 2). This synthesis involved combining *trans*-(i-$Pr_3P)_2$(4-FC_6H_4)Pd(I) (**8**) with 3.0 equivalents of thallium 4-fluorophenylboronate (**10**) in the presence of dibenzo-22-crown-6 (*32*), together with 1.0 equivalent of i-Pr_3P in THF, at –78°C; this was followed by warming to –30°C in the NMR spectrometer (Fig. 2). A small amount of conversion (~10%) to complex **11** was observed, together with cross-coupling product **13** (~30%), by ^{31}P and ^{19}F NMR spectroscopy, demonstrating that intermediate **11** can be formed without the intermediacy of arylpalladium hydroxide complexes (*33*).

To support the assertion that the boron atom in **11** is tricoordinate (6-B-3), a second independent synthesis of **11** was undertaken (route 3). A solution of arylpalladium hydroxide complex **6** and 4-fluorophenylboroxine **12** (0.33 equivalents) in THF-d_8 was combined with 2.0 equivalents of i-Pr_3P at –78°C in an NMR tube, which was quickly inserted into the NMR spectrometer that had been pre-cooled to –60°C, whereupon complex **11** was observed (Fig. 2, route 3). A ~50% conversion to **11** was observed at –60°C over 36 hours, along with cross-coupling product **13**. The similarity of the spectroscopic data (including the NOE spectroscopy cross peaks and the ^{11}B NMR chemical shifts; figs. S13 to S21) for the species generated from the three independent syntheses provides compelling support for the structural assignment of **11** as a 6-B-3 palladium(II) complex containing a Pd-O-B linkage.

The formation of 6-B-3 complex **11** must proceed via an 8-B-4 complex (such as **3**; Fig. 1) that is formed initially which then suffers by the rapid loss of a molecule of water. We attempted to shift the equilibrium toward such a complex by generating **11** in mixtures of THF and H_2O (99:1), but we observed no change in the ^{31}P, ^{19}F, or ^{11}B NMR spectra. We considered exploring more strongly coordinating hydroxide sources that are often used in Suzuki-Miyaura reactions, but the addition of inorganic bases to THF-H_2O blends is known to form biphasic mixtures (*13*). Fortunately, CsOH•H_2O dissolves readily at –30°C in mixtures of THF and CH_3OH (12:1). A freshly generated sample of 6-B-3 complex **11** (from **6** and **7;** vide supra) at 0.034 M in THF was cooled to –78°C; this was followed by the addition of 50 μl of a 2 M solution (5.0 equivalents) of CsOH•H_2O in methanol. The sample was monitored by NMR spectroscopy at –30°C, but again, no change in the ^{19}F, ^{31}P, or ^{11}B NMR spectra was observed.

The resistance of the boron atom in complex **11** to adopt a tetracoordinate geometry is probably caused by the steric hindrance that results from the presence of two i-Pr_3P ligands on the palladium atom (F- and B-strain) (*34*). Thus, to enable saturation of the boron valences would require a decrease in steric congestion, achieved by

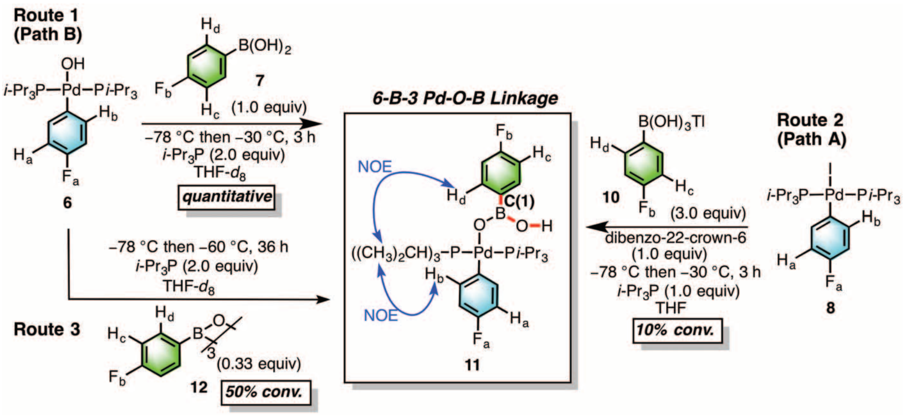

Fig. 2. Formation of a 6-B-3 complex containing a Pd-O-B linkage. The crossing lines for compound **12** signify a cyclic trimer. In the middle panel, the red bonds indicate HMBC cross peaks. Throughout, h indicates hours; equiv, equivalents; conv., conversion; quantitative, 100% conv.

removing a *i*-Pr$_3$P ligand from arylpalladium hydroxide complex **6**. This hypothesis led to the investigation of monoligated arylpalladium hydroxy complex, [(*i*-Pr$_3$P)(4-FC$_6$H$_4$)Pd(OH)]$_2$ (**17**), which exists in dimeric form in both solution and solid states (*35*).

The addition of a THF-d_8 solution of **7** (2.0 equivalents) to a THF-d_8 solution of **17** (1.0 equivalent) at −78°C, followed by warming to −60°C, produced no new complexes. However, upon cooling the solution to −100°C, a new species emerged, with complete consumption of **17** and with 50% of **7** remaining (Fig. 3, route 4). The structure of this species could be assigned as the bridged *bis*-arylpalladium arylboronate complex (**18**), which is reminiscent of other palladium acetate and carbonate complexes (*36*, *37*). The stoichiometry of complex **18** was determined by adding a THF-d_8 solution of **7** (1.0 equivalent) to a THF-d_8 solution of **17** (1.0 equivalent) at −60°C, followed by cooling to −100°C, where a quantitative conversion was observed. This dinuclear complex did not incorporate another molecule of **7**, even in the presence of 3 additional equivalents of **7** at −100°C. However, exchange spectroscopy showed cross peaks between **18** and unbound **7** at −100°C, demonstrating that the system was in equilibrium even at this temperature. This stoichiometry (1B:2Pd) is attributed to the thermochemical preference for Pd-(μ-OH)-Pd moieties, which is observed in other bridged mixed-hydroxide complexes (*38*).

The connectivity of the Pd-O-B linkage in **18** was confirmed by the observation of NOEs between H$_b$, H$_d$, and the bridging OH group with the methyl hydrogens on the *i*-Pr$_3$P group. The observation of NOE cross peaks, along with HMBC ($^3J_{\text{BOH-C(1)}}$) cross peaks between the BOH and the *ipso*-carbon–bearing boron (red bonds), indicates that the arylboronic acid and arylpalladium hydroxide are connected. The ^{11}B NMR chemical shift of **18** was too broad to determine accurately. The broadening of the ^{11}B NMR signal in complex **18** is probably attributable to the chemical exchange between **7** and **18**.

To further aid in the structure determination of **18**, we combined 3.0 equivalents of thallium arylboronate **10** with [(*i*-Pr$_3$P)(4-FC$_6$H$_4$)Pd(I)]$_2$ (**19**) in THF-d_8 at −78°C and then warmed the sample to −50°C (Fig. 3, route 5). Cooling the mixture to −100°C resulted in the observation of complex **18** (~50%) by ^{1}H NMR spectroscopy. The ability to forge the Pd-O-B linkage in **18** by two routes provides compelling support for the structural assignment.

In an attempt to arrive at a different stoichiometry (1B:1Pd), 60 μl of CH$_3$OH was injected into a THF-d_8 solution of **18** with 1.0 equivalent of **7** (from **17** and **7**; vide supra), which resulted in the quantitative formation of a new species (**20**) (Fig. 3). The presence of a Pd-O-B linkage in **20** was established by the observation of NOE cross peaks between the methyl hydrogens on the *i*-Pr$_3$P and both H$_b$ and H$_d$ (Fig. 3, blue arrows, and fig. S57). The ^{11}B NMR chemical shift of **20** at 9 ppm is well within the characteristic chemical shift regime of tetracoordinate (8-B-4) complexes (*12*, *13*, *39*). The proposed Pd-O-B-O core can be found in an analogous bridging arylpalladium acetate complex (*40*, *41*).

The ability to generate intermediate species containing Pd-O-B linkages provided a singular opportunity to examine the kinetic aspects of the transmetalation event in the Suzuki-Miyaura cross-coupling reaction. The transfer of the aryl group from boron to palladium was investigated by using NMR spectroscopy to follow the decay of complex **20** and the concomitant formation of cross-coupling product **13**.

The addition of CH$_3$OH into a THF solution of **18** and **7** at −55°C led to the generation of **20**. The subsequent formation of cross-coupling product **13** was monitored by ^{19}F NMR spectroscopy at −30°C (to expedite data collection). First-order plots of [**20**] and [**13**] versus time (figs. S62 to S64) were fitted by using the functions [A] = [A]$_0e^{-kt}$ and [P] = [A]$_0$(1 − e^{-kt}), respectively, where [A] is the concentration of **20**, [A]$_0$ is the initial concentration of **20**, [P] is the concentration of **13**, k is the rate constant, and t is time. These functions provided accurate values for k_{obs} (the observed kinetic constant) for the decay of **20** [(1.41 ± 0.02) × 10^{-3} s^{-1}] and the formation of **13** [(1.55 ± 0.09) × 10^{-3} s^{-1}; Fig. 4A].

A similar kinetic analysis was performed in pure THF by combining a THF solution of **7** (2.0 equivalents) with a THF solution of **17** (1.0 equivalent) at −78°C, followed by warming the sample to −30°C. First-order decay of arylpalladium complex **18** and the formation of **13** were observed with k_{obs} values of (7.59 ± 0.58) × 10^{-4} s^{-1} and (5.78 ± 0.13) × 10^{-4} s^{-1}, respectively (figs. S65 to S67), indicating that the decay of **18** and the formation of **13** coincide. The correspondence of these rate constants and the clean first-order behavior suggests that at −30°C, **18** is largely converted to **20** (sufficient **7** is present to allow this) (*42*). Moreover, the similarity of the rate constants in THF and the THF-CH$_3$OH mixture further supports the conclusion that **18** is converted to **20** before transmetalation (Fig. 4A) (*43*).

The generation of 6-B-3 complex **11**, with its Pd-O-B linkage, raised the question of whether this complex is a competent intermediate in the Suzuki-Miyaura reaction. Complex **11** was thermally stable at −30°C in the presence of an excess of *i*-Pr$_3$P for over 24 hours, indicating that added phosphine attenuates the rate of the transmetalation process. A THF solution of this complex was warmed from −30°C in 10°C intervals, whereupon a

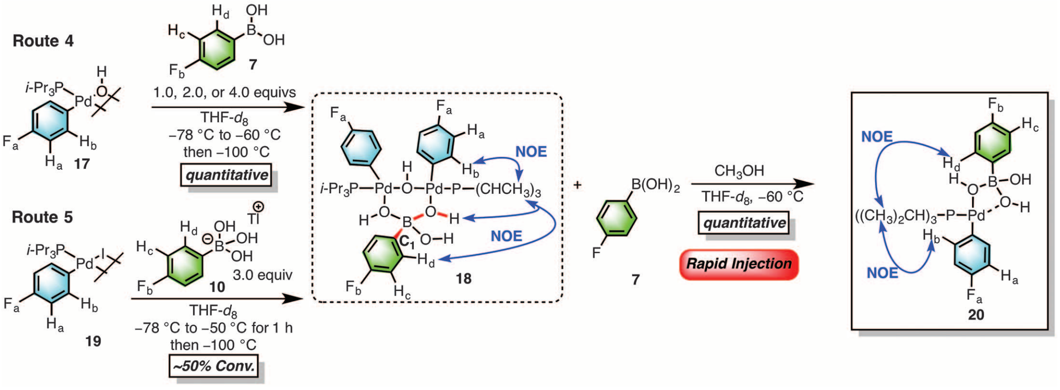

Fig. 3. Formation of 8-B-4 complexes containing Pd-O-B linkages.

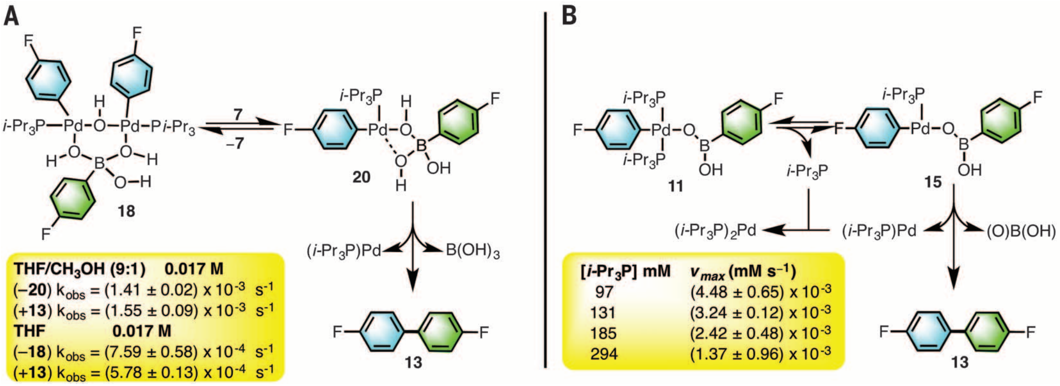

THF/CH$_3$OH (9:1) 0.017 M
(**−20**) $k_{obs} = (1.41 \pm 0.02) \times 10^{-3}$ s^{-1}
(**+13**) $k_{obs} = (1.55 \pm 0.09) \times 10^{-3}$ s^{-1}
THF 0.017 M
(**−18**) $k_{obs} = (7.59 \pm 0.58) \times 10^{-4}$ s^{-1}
(**+13**) $k_{obs} = (5.78 \pm 0.13) \times 10^{-4}$ s^{-1}

[*i*-Pr$_3$P] mM	**v_{max} (mM s^{-1})**
97	$(4.48 \pm 0.65) \times 10^{-3}$
131	$(3.24 \pm 0.12) \times 10^{-3}$
185	$(2.42 \pm 0.48) \times 10^{-3}$
294	$(1.37 \pm 0.96) \times 10^{-3}$

Fig. 4. Kinetic data. (**A**) Formation of **13** from 8-B-4 complexes **18** and **20** (negative signs indicate consumption of starting material). (**B**) Inverse order dependence on [*i*-Pr$_3$P] for the formation of **13** from 6-B-3 complex **11**.

considerable amount of cross-coupling product **13** was observed by means of ^{19}F NMR spectroscopy at 20°C over the course of 3 to 12 hours. A plot of [**11**] versus time displayed s-shaped curves (figs. S68 to S91), signifying that the k_{obs} increases during the course of the reaction (which is indicative of autocatalysis) (*44*).

To confirm the kinetic requirement for phosphine dissociation in the cross-coupling of **11**, the kinetic order in phosphine was determined by adding a THF solution of **7** to a solution of **6** with increasing amounts of *i*-Pr$_3$P, ranging from 97 to 294 mM, at 20°C (Fig. 4B). The s-shaped kinetic profiles were fitted, and a v_{max} (maximum rate) was extracted from the data (*45*). A plot of log[v_{max}] versus log[*i*-Pr$_3$P] gave a slope of –1.05 ± 0.05 (fig. S92), which is consistent with an inverse dependence on phosphine, indicating that dissociation of a phosphine is a pre-equilibrium process that leads to the hypothetical 14-electron palladium complex **15**. Because **15** is formed in such a low-equilibrium concentration, it is not possible to determine whether transmetalation occurs directly from this 6-B-3 species or whether it requires the coordination of another group on boron to form species related to **20**. Although very low levels of halide and water are present, the coordination state of boron in the transmetalation event cannot be unambiguously established.

Through the combination of three methods of investigation (spectroscopic analyses, independent syntheses, and kinetic measurements), we have unambiguously identified and characterized three pre-transmetalation species containing Pd-O-B linkages that undergo the Suzuki-Miyaura cross-coupling reaction. Despite the long-held assumption that these types of intermediates are involved in the transmetalation event, our study provides the first definitive evidence for their involvement. We have demonstrated that both tetracoordinate (**18** and **20**) and tricoordinate (**11**) boron complexes containing the critical Pd-O-B moieties are able to transfer their B-aryl groups to palladium. Moreover, our investigations establish that an empty coordination site on the palladium atom is needed for the transmetalation event to take place from all three Pd-O-B–containing species. We foresee these results serving as a platform for further investigations of the venerable Suzuki-Miyaura cross-coupling process.

REFERENCES AND NOTES

1. F. Chemla, F. Ferriera, A. Perez-Luna, L. Micouin, O. Jackowski, in *Metal-Catalyzed Cross-Coupling Reactions and More*, A. de Meijere, S. Bräse, M. Oestreich, Eds. (Wiley-VCH, ed. 3, vol. 1, 2014), chap. 5, pp. 365–422.
2. J. C. H. Lee, D. G. Hall, in *Metal-Catalyzed Cross-Coupling Reactions and More*, A. de Meijere, S. Bräse, M. Oesteich, Eds. (Wiley-VCH, ed. 3, vol. 1, 2014), chap. 2, pp. 65–132.
3. B. Martín-Matute, K. J. Szabó, T. N. Mitchell, in *Metal-Catalyzed Cross-Coupling Reactions and More,* A. de Meijere, S. Bräse, M. Oestreich, Eds. (Wiley-VCH, Weinheim, ed. 3, vol. 1, 2014), chap. 6, pp. 423–465.
4. S. Xu, H. Kamada, E. H. Kim, A. Oda, E. Negishi, in *Metal-Catalyzed Cross-Coupling Reactions and More,* A. de Meijere, S. Bräse, M. Oestreich, Eds. (Wiley-VCH, Weinheim, ed. 3, vol. 1, 2014), chap. 3, pp. 133–278.
5. W. T. T. Chang *et al.*, *Org. React.* **75**, 213–746 (2011).
6. A. Suzuki, *Angew. Chem. Int. Ed.* **50**, 6722–6737 (2011).
7. A. Suzuki, *J. Organomet. Chem.* **576**, 147–168 (1999).
8. C. Valente, M. Organ, in *Boronic Acids: Preparation and Applications in Organic Synthesis and Medicine*, D. G. Hall, Ed. (Wiley-VCH, vol. 2, 2005), chap. 4, pp. 213–262.
9. J. Liu, J. J. Lavigne, in *Boronic Acids: Preparation and Applications in Organic Synthesis and Medicine*, D. G. Hall, Ed. (Wiley-VCH, vol. 2, 2005), chap. 14, pp. 612–676.
10. B. Matthias, H. U. Blaser, Eds., *Organometallics as Catalysts in the Fine Chemical Industry*, vol. 42 of *Topics in Organometallic Chemistry* (Springer-Berlin, 2013).
11. J. Magano, J. R. Dunetz, *Chem. Rev.* **111**, 2177–2250 (2011).
12. K. Matos, J. A. Soderquist, *J. Org. Chem.* **63**, 461–470 (1998).
13. B. P. Carrow, J. F. Hartwig, *J. Am. Chem. Soc.* **133**, 2116–2119 (2011).
14. C. Amatore *et al.*, *Chemistry* **17**, 2492–2503 (2011).
15. C. Amatore *et al.*, *Chemistry* **18**, 6616–6625 (2012).
16. C. Amatore *et al.*, *Chemistry* **19**, 10082–10093 (2013).
17. A. F. Schmidt *et al.*, *Russ. J. Gen. Chem.* **81**, 1573 (2011).
18. A. F. Schmidt, A. A. Kurokhtina, *Kinet. Catal.* **53**, 714–730 (2012).
19. A. O. Aliprantis, J. W. Canary, *J. Am. Chem. Soc.* **116**, 6985–6986 (1994).
20. C. Sicre *et al.*, *Tetrahedron* **64**, 7437–7443 (2008).
21. N. Miyaura, A. Suzuki, *J. Chem. Soc. Chem. Commun.* **1979**, 866–867 (1979).
22. A. J. J. Lennox, G. C. Lloyd-Jones, *Angew. Chem. Int. Ed.* **52**, 7362–7370 (2013).
23. J. F. McGarrity, J. Prodolliet, *J. Org. Chem.* **49**, 4465–4470 (1984).
24. S. E. Denmark, B. J. Williams, B. M. Eklov, S. M. Pham, G. L. Beutner, *J. Org. Chem.* **75**, 5558–5572 (2010).
25. Although *i*-Pr$_3$P is not commonly used in Suzuki-Miyaura reactions, it is structurally similar to *c*-Hex$_3$P (*c*-Hex, cyclohexyl), which has widespread application (*2, 26*).
26. G. C. Fu, *Acc. Chem. Res.* **41**, 1555–1564 (2008).
27. Y. Nishihara, H. Onodera, K. Osakada, *Chem. Commun. (Camb.)* **2004**, 192–193 (2004).
28. This nomenclature designates an N-X-L species, where N is the number of formally valence-shell electrons around atom X that are involved in bonding L ligands to X (*29*).
29. C. W. Perkins *et al.*, *J. Am. Chem. Soc.* **102**, 7753–7759 (1980).
30. K. Osakada, H. Onodera, Y. Nishihara, *Organometallics* **24**, 3815–3817 (2005).
31. P. Zhao, C. D. Incarvito, J. F. Hartwig, *J. Am. Chem. Soc.* **129**, 1876–1877 (2007).
32. E. Weber, K. Skobridis, M. Ouchi, T. Hakushi, Y. Inoue, *Bull. Chem. Soc. Jpn.* **63**, 3670–3677 (1990).
33. We cannot unambiguously exclude the possibility that thallium hydroxide dissociates to a minor extent, forming the palladium hydroxide complex **6**. These results do not contradict the conclusions of the studies led by Hartwig (*13*) and Amatore and Jutand (*14–16*). The kinetic incompetence of sodium or potassium boronates in aqueous-organic solutions need not carry over to organic-only solutions of thallium boronates.
34. H. C. Brown, *J. Am. Chem. Soc.* **67**, 374–378 (1945).
35. V. V. Grushin, H. Alper, *Organometallics* **15**, 5242–5245 (1996).
36. T. A. Stephenson, S. M. Morehouse, A. R. Powell, J. P. Heffer, G. Wilkinson, *J. Chem. Soc.* 3632–3640 (1965).
37. C. S. Wei *et al.*, *Angew. Chem. Int. Ed.* **52**, 5822–5826 (2013).
38. M. S. Driver, J. F. Hartwig, *Organometallics* **16**, 5706–5715 (1997).
39. H. Nöth, B. Wrackmeyer, in *Nuclear Magnetic Resonance Spectroscopy of Boron Compounds*, P. Diehl, E. Fluck, R. Kosfeld, Eds., vol. 14 of *NMR Basic Principles and Progress* (Springer-Verlag, 1978), chap. 7, pp. 74–100.
40. Y. Tan, F. Barrios-Landeros, J. F. Hartwig, *J. Am. Chem. Soc.* **134**, 3683–3686 (2012).
41. We cannot unambiguously exclude the possibility that methanol has incorporated into complex **20**.
42. Although **18** and **7** are both observed at −100°C, at −30°C, these species converge, thus preventing a definitive assignment of whether **18** or **20** is the actual species undergoing decay in the kinetic analysis.
43. M. Wakioka, Y. Nakamura, Q. Wang, F. Ozawa, *Organometallics* **31**, 4810–4816 (2012).
44. The identity of the species that is inducing autocatalysis has not been determined at this time.
45. R. Schmid, V. N. Sapunov, *Non-Formal Kinetics: In Search for Chemical Reaction Pathways*, vol. 14 of *Monographs in Modern Chemistry*, H. F. Ebel, Ed. (Verlag Chemie, 1982).

ACKNOWLEDGMENTS

We are grateful for generous financial support from the NSF (CHE-1012663 and CHE-1151566). A.A.T. is grateful to the University of Illinois for graduate fellowships. We thank L. Zhu for helpful suggestions regarding NMR spectroscopy. Some of the data presented here were collected in the Core Facilities of the Carl R. Woese Institute for Genomic Biology on a 600-MHz NMR instrument (funded by NIH grant S10-RR028833) or at the Integrated Molecular Structure Education and Research Center at Northwestern University. Full experimental procedures, characterization and kinetic data, and copies of the ^{1}H, ^{13}C, ^{31}P, ^{19}F, ^{11}B, NOE, and exchange spectra can be found in the supplementary materials.

SUPPLEMENTARY MATERIALS

www.sciencemag.org/content/352/6283/329/suppl/DC1
Materials and Methods
Figs. S1 to S118
Tables S1 to S26
References (*46–51*)

28 October 2015; accepted 23 February 2016
10.1126/science.aad6981